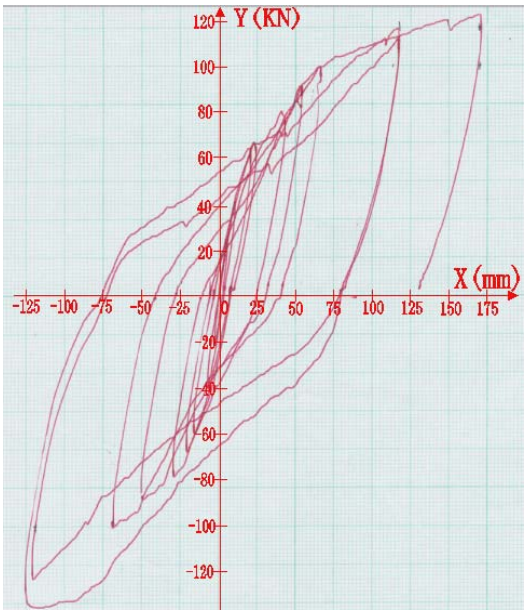

(a) KJ1

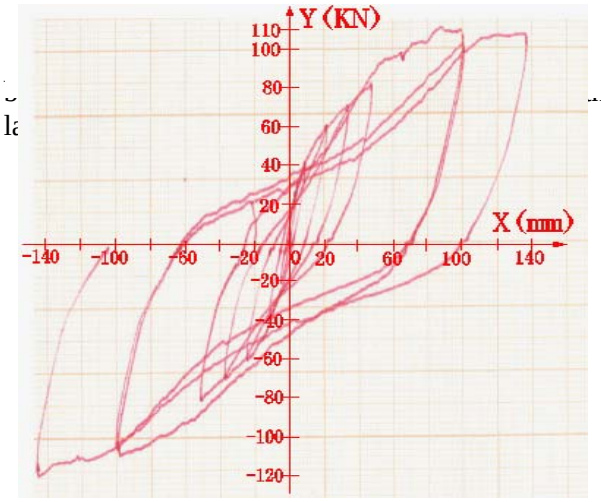

(b) KJ2

Fig.14 load-displacement hysteresis loops of KJ1 and KJ2

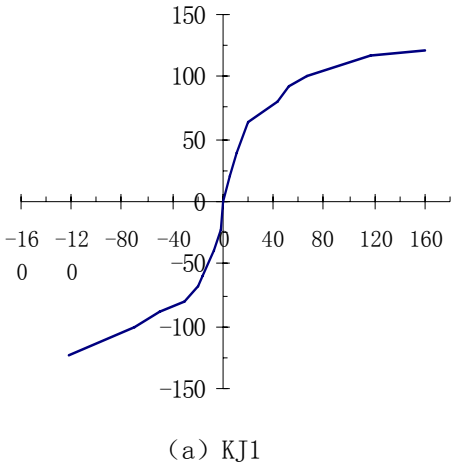

(a) KJ1

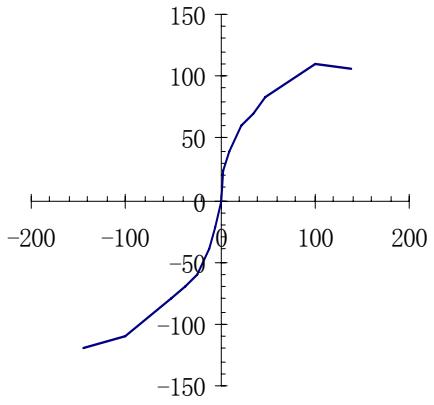

(b) KJ2

Fig .15 Envelope of the cyclic response of specimens

Table 4 some experimental results

Specimen	Yield load (kN)	Yield displacement (mm)	maximum load (kN)	Maximum load (mm)	the ductility coefficient	the initial stiffness (kN/mm)
KJ1	80/-80	43/-30	122/-135	170/-125	3.95/4.16	6.94
KJ2	70/-70	34/-38	110/-120	110/-146	3.2/3.84	5.0

Fig.15 was the envelop of the cyclic response of KJ1 and KJ2 respectively. The relations of moment and rotation were outlined. The line relations of moment and rotation were showed in the initial phase and the phase was very short. With increasing the load, the noalinear relations of moment and rotation became very apparent. The fluctuating phenomenon of the relations was revealed. The main reason was that the In seismic design, cyclic energy dissipation is of great important, since it expresses the ability of the members and their connections to dissipate earthquake input energy. Generally, sufficient energy dissipation without substantial loss of strength and

stiffness constitutes desirable behavior for beam-column subassemblages. It was confirmed that most of the energy was dissipated in the flange of top-seat angles while the column and web angles participated a little in the energy dissipation process in this test.

3.7.2 The analysis of the hysteresis secialitys

It can be seen from the hysteresis loops, all the models have better tensility. In actually measured curves, which the frame KJ-1 and KJ-2 of top-seat and two web angles connection were much full, that means their performance of absorbing wre advantage to seismic. According to seismic code, the energy-consuming factor of different kinds of the frame in various stages was calculated, as Table 5 shown. It can be seen from Table 5, From the yielding at begin to the third yield displacement, the energy-consuming factor of the frame was growing, that was to say that of the model frame was growing in a certain range. In addition, the increasing trend of the energy-consuming factor of KJ-2 was obvious, that means the late energy performance of KJ-2 was better. intermediate stage appearing obvious furling phenomena, That was mainly because there was some slippage between the beam chord and connecting angle steel, and the bolts preload minished gradually under the reciprocating loads.

It can be gained from the skeleton curves shown in Fig 6.14, they were not slick, because the gap among linkers, bolts, columns and beams when machining and making the specimens, which can bring certain slippage, and put up dithering on the hysteresis loops and skeleton curves. The linear stage of the two frames KJ-1 and KJ-2 presented was very short in the initial stage of loading, when the loads reached 60KN, non-linearity appeared because of the obvious yield of the connecting angle steel, and result in frame connecting yield when enduring smaller loads.

In the course of loading, according to the test phenomena and strain value gained from the strain gages, much energy that KJ-1 and KJ-2 absorbed was dissipated by the deformation of the connecting angle steel, little was dissipated by the beam and column chord of the connections.

It can be seen From all levels of hysteresis loop diagonal angle decreases, that stiffness of specimens lost after came into the plastic, which was mainly because of the plastic deformation of connected angle and the slippage of high strength bolts in keyhole. This phenomenon has significantly changed the shape of hysteresis loop. According to seismic code, the lateral rigidity of the frame was calculated, and the stiffness curve of the model frame in every loading stages was drawn. (Fig.16). As can be seen from the Fig.16, the stiffness of KJ-1 and KJ-2 were smaller, and anti-lateral performance were better.

Table 5
dissipation coefficient in every stage

Frame types	dissipation coefficient in every stage					
	yield	$1\Delta_c^1$	$1\Delta_c^2$	$2\Delta_c^1$	$2\Delta_c^2$	$3\Delta_c^1$
KJ-1	1.132	1.305	1.602	1.650	-	-
KJ-2	0.96	1.374	1.262	1.401	-	-

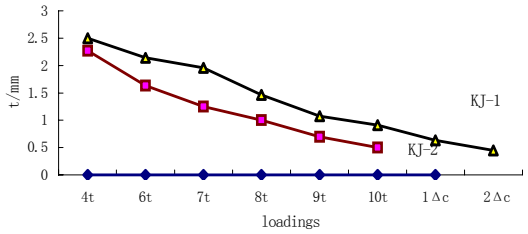

Fig.16 stiffness of the frame

Tensility coefficient is the ratio of the ultimate displacement Δ_u and yield displacement Δ_y when the frame destructed, namely $\mu = \Delta_u / \Delta_y$, and this test did not come to ultimate displacement Δ_u, so there was no tensility coefficient. But the ratio of the largest displacement Δ_{max} and yield displacement Δ_y was as follows shown:

$$\mu \geq \Delta_{max} / \Delta_y = 135/20 = 6.75 \quad \text{(KJ-1)}$$

$$\mu \geq \Delta_{max} / \Delta_y \geq 100/22 = 4.54 \quad \text{(KJ-2)}$$

Seismic Design specifications requires the framework tensility coefficient factor $\mu \geq 4.0$, and it could be obtained that tensility coefficients of two types of steel frame were satisfied. That was to say that the steel frame had good anti-seismic capacity.

3.7.3 Moment and rotation angle analysis

According to two Electrical and Mechanical centesimal meters tables 1 and 2, the rotation angles of beams and columns were calculated. The beam end moments were calculated by analyzing the strain value.

After analysis, the relation between Bending moment and rotation angle can be drawn, as shown in Figure 6.16.

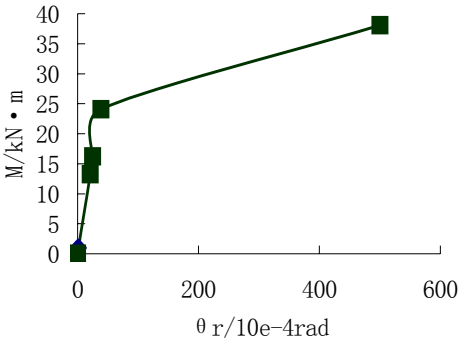

Fig.17 the relation between bending moment and rotation angle

3.7.4 plastic hinge analysis

Because the strain gages could not be pasted on the angles of the semi-rigid connections in KJ-1 and KJ-2, the strain value could not be gained in different loading stages. At the same time, larger deformation of the angles could be observed in the testing, That was to say the angle was more flexible, and making beam ends suffered smaller moment, so there was no plastic hinge appeared on beam ends. According to the yield phenomenon gained from the analysis of strain values, this occured only in the side-angle chord had also proved this point. Semi-rigid steel frame was difficult to meet the " strong nodes and weak components" of the seismic design requirements. According to the strain gages, the time and order plastic hinges could also be found, as shown in Fig.18. As can be seen from the Fig.18, plastic hinge first appeared in the beam ends, and later in the column ends, which satisfying "strong columns and weak beams" of the design requirements.

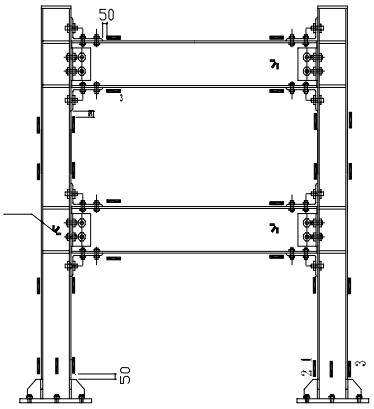

Fig.18 the yield order of each frame in loading stage

4 Finite element analysis

4.1 establishment of finite element model and matrrial paramenters

The mode of KJ-1 is established and analyzed by ANSYS. The finite element model of KJ-1 is showed as Fig.19 in which steel frame is divided into beam119 elements.

The stress-strain relation curve of steel is decided by actural testing result of matetials. Other material parameters are listed as following: the elastic modulus of steel is 1.9793 × 105Mpa, and the Poisson's ratio of steel is 0.27.

4.2 computation results

Through the finite element computation, the load-displacement hysteresis loops, the curve of load-angle relation of top-seat and two web angles connections, the skeleton curve of load-displacement relation, the curve of degeneration of rigidity, the equivalent stress contours under yield and ultimate loads and other results of KJ1 are obtained here shown in Fig.19-22.

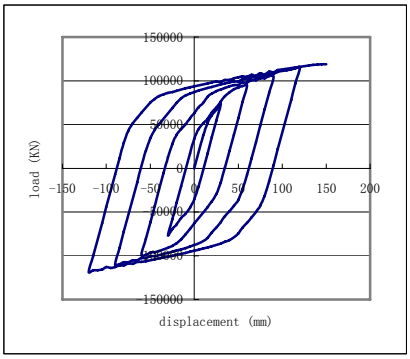

Fig 19 load-displacement hysteresis loops

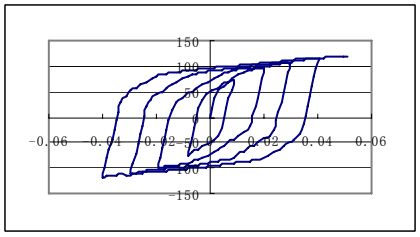

Fig 20 load-angle hysteresis loops

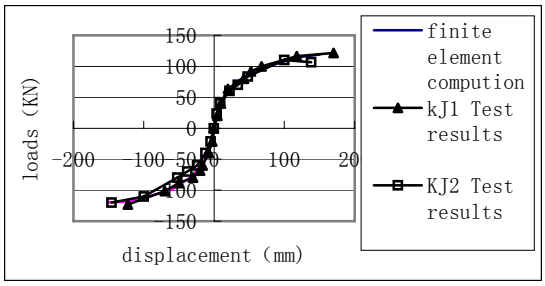

Fig.21 comparison of envelope between finite element and test

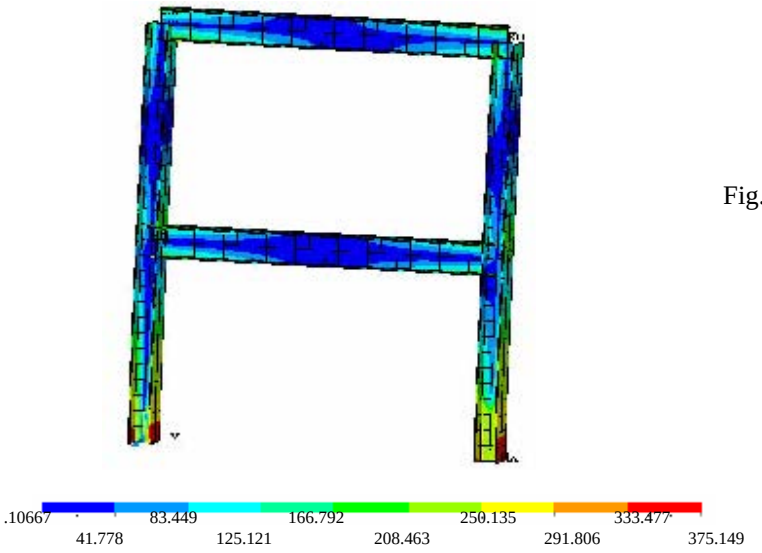

Fig.22 the last deformation figure of steel frame

Fig.19 and Fig.20 demonstrat that the computation results by finite element method accord with the experimental ones well. Because of the limitation of experimental loading equipment, the plastic hinge does not form in frame, so that latter phase of load-displacement curve connot be got, but the front part coincides with the computation curve very well. Fig 8 also indiates that steel frame with semi-rigid connections can possess the relative high stiffness, strength and excellent ductility, because of the better deformation ability of top-seat and two web angles connections.

Fig.20 shows that envelope curves between finite element computation and test are very similar, so the finite element computation results are reliable.

Figure 10 shows the deformation and equivalent stresss contours of frame when horizontal load is increased 115KN. Some results show that the maxium horizontal displacement of beam in upper story of frame is 172.327mm, the maxium stress is 375.149 KN/m^2. With the increase of load, the plastic area extend to bottom of column, and form a plastic hinge in bottom of column. At last when a plastic hinge is formed in every bottom of column in frame, the frame becomes a mechanism so the computation is finished, as showed in Fig.23 and Fig.24. This demonstrat that the computation results by finite element method accord with the experimental ones well.

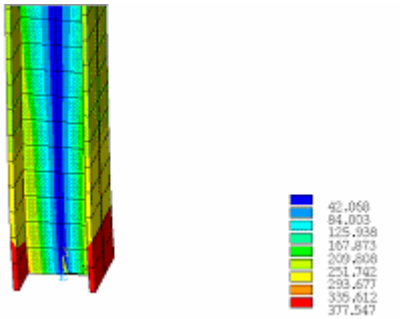

Fig.23 equivalent stress contours of left column botton under ultimate load

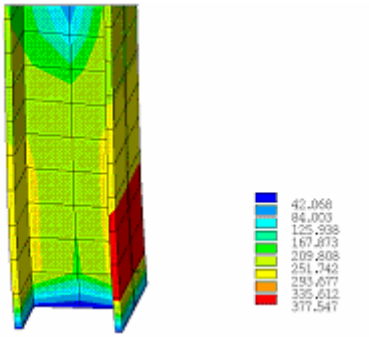

Fig.24 equivalent stress contours of right column botton under ultimate load

5 Conclusions

It was confirmed that most of the energy was dissipated in the flange of top-seat angles while the column and web angles participated a little in the energy dissipation process in this test.

The experimental research and finite element analysis on steel frame structure with semi-rigid connections show that a significant extent lateral resistant rigidity, ability of energy consumption and ductility of this structural system are better than common steel rigid frame structural system.

Referrences.

[1]C. Bernuzzi, R. Zandonini and P. Zanon. Experimental analysis and modeling of semi-rigid steel joints under cyclic reversal loading.Construct. Steel Research[J], vol.38. Fubruary 1996.pp.95～123,

[2]E. M. Lui and W-F. Chen, Analysis and behavior of flexibly-jointed frames, Engineering and Structure, Vol.8, April ,1986.pp: 107-118

[3]K.S.Sivakumaran, Seismic response of multi-storey steel buildings with flexible connections, Engineering and Structure, Vol.10, October1988,pp: 239-247

[4]Hsieh S-H , Deierlein, Nonlinear analysis of three-dimensional steel frames with semi-rigid

connections.Computers and Structures[J], v41(5) 1991, pp:995-1009.
[5]Seung-Eock Kim, Kyung-Won Kang .Large-scale testing of 3-D steel frame accounting for local buckling . International Journal of Solids and Structures [J], V41,(18-19) 2004,pp: 5003-5022.